Space-time QAM wireless MISO systems employing differentially coded in-/out-FECC SCQICs over slow-fading Jakes scattering mobile radio links

Ardavan Rahimian[1], *Farhad Mehran*[1], *Robert G. Maunder*[2]

[1]*School of Electronic, Electrical and Computer Engineering, University of Birmingham, Birmingham B15 2TT, UK*
[2]*School of Electronics and Computer Science, University of Southampton, Southampton SO17 1BJ, UK*
E-mail: rahimian@ieee.org

Published in *The Journal of Engineering*; Received on 2nd January 2014; Accepted on 1st July 2014

Abstract: This study presents research that supplements and extends the previous works on design of space-time fully systematic unpunctured (FSU) serial concatenation of quadratic interleaved codes (SCQICs). The requirements for efficient design of the forward error correction (FEC) codecs motivated potential information-theoretic studies for enjoying the development of low-complex system components within the FEC encoder/decoder for securing the transmission reliability. Inspired by this motivation, this study not only provides design guidelines to achieve better bit error rate performance in terms of the major design factors of FSU-SCQICs, that is, component code constraint length and trellis structure, and FEC rate, but also estimates the gain gaps of different quadratic permutation (QP) structures in two crucial untouched aspects: (i) signal-to-noise ratio-region comparison on the optimality and (ii) investigation on the structural parameters of QPs, that is, cyclic shift and primitive factor.

1 Introduction

One of the most important design issues concerning research studies on the space-time turbo codes (STTCs) [1] aims to improve the key performance factors that have direct determinant effect on the overall bit error rate (BER) performance. Hence, it is vital to design the effective permutation arrays in regard to a waterfall-region of the BER curve and the region that exhibits a much shallower slope, that is, flare region. In particular, for the STTCs that enjoy cascaded systematic recursive convolutional codes (SRCCs) for yielding relatively high minimum distance, interleaver design issues are not reaching the state of maturity [2]. From theoretical design aspects, algebraic constructions are attracting particular interest for performing the scrambling/unscrambling functions since they yield provisioning coding gain in critical regions of the BER performance curve and enable possibility of analysis and compact representation. An additional enhancement which opens the way for their practical utilisation is their considerable lower implementation complexities.

2 Research contribution

It has been previously shown that serial turbo-like codes employing the quadratic permutations (QPs), that is, the serial concatenation of quadratic interleaved codes (SCQICs), result in outstanding coding gains [3–6]. This paper aims to supplement and extend the pivotal system design guidelines of our previous works in order to achieve a flexible SCQIC framework in terms of other crucial contradictory performance factors, so as to address the proposed SCQICs in co-operation with the highly matured technologies (e.g. bit-level space-time codes) employing the high-throughput modulation along with other specified features; which have been briefly outlined as follows:

(1) *Component code structure*: Inspired by the motivation of finding promising generator polynomials which result in maximisation of component code minimum free distance [7]; this paper investigates the gain gap limits between provisioning choices of the convolutional component code (CCC) trellis structures for different feasible constraint lengths, with respect to the tolerable incurred decoding complexity, that is, the widely used range $L \leq 5$.
(2) *FEC rate*: In terms of providing both coding gains and spectral efficiencies, flexible FEC code rate enables adaptation of provision signal-to-noise ratio (SNR) operating point (which yields minimal BER) with respect to the bandwidth limitations of wireless channels. Hence, the investigation has been further broadened for lower code rates than typical 0.33, which is widely used for wireless transmissions.
(3) *Differential coding (DC) inside-/outside-forward error correction codec (FECC)*: There exist a wide range of advantages and disadvantages as a result of employing DC as the phase-ambiguity resolution technique [8] for high-throughput widely used 16-quadrature amplitude modulation (QAM) transmissions. One important issue of great theoretical and practical interest is to gain the benefits of DC technique while avoiding unnecessary BER degradation (because of the double-error phenomenon) by applying the DC external to the FECC, rather than modulating differentially coded version of FECC, that is, DC inside-FECC [9]. The studies (1) and (2) of this outlined list are supplemented by comparing the sacrificed gain gaps with respect to employing DC internal or external to FECC or the same system model based on the coherent detection.
(4) *Optimality on SNR region(s)*: Studies on comparison of different permutation algorithms to be employed in FEC-coded systems reveal that the superior BER performance of the selected one may yield inferior performance as interleaver size changes significantly. For example, for the parallel concatenated convolutional coding (PCCCing), although pseudo-random interleavers have been shown to have superior performance to the block interleavers for the large frame lengths, in many cases their inferior performance in the low frame sizes has been confirmed [10]. Hence, the inevitable investigation for the gain gaps between SCQICs with respect to reference of comparison, that is, the same system using randomly generated scramblers/unscramblers, are carried out in order to ensure that the gap is not significant; i.e. not yielding unexpected high probability of bit error and hence changing the unexpected level of optimality in particular SNR region.
(5) *Structural parameters of QPs*: Monte Carlo computer simulations have been conducted in order to potentially predict the performance of SCQICing when the QP-vectors utilise different multiplicative factors and cycle shifts.

The system investigations have been thoroughly conducted in a rich isotropic scattering mobile radio channel based on the Jakes

This is an open access article published by the IET under the Creative Commons Attribution License (http://creativecommons.org/licenses/by/3.0/)

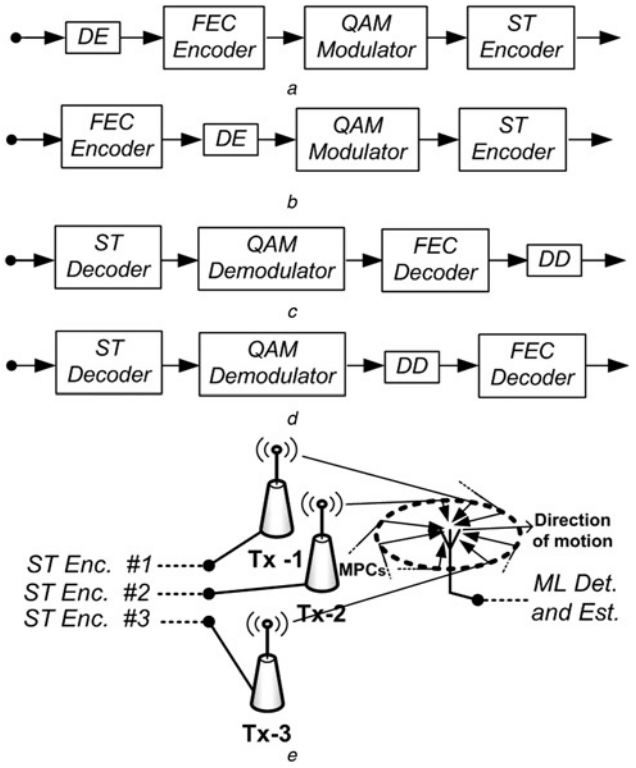

Fig. 1 *STTC encoder/decoder*
a External-FECC-DC SCQIC encoder
b Internal-FECC-DC SCQIC encoder
c DD-out-FECC iterative SCQIC decoder
d DD-in-FECC iterative SCQIC decoder
e Conceptual representation of Jakes scattering wireless MISO mobile radio link

Doppler power spectrum [11]; that is, where a scatter ring is placed around the receiver in order to model and analyse the multipath components, and the isotropic continuum of arriving components is approximated by the plane radiowaves arriving at the uniformly spaced azimuthal angles.

3 Wireless system model

3.1 STTC encoder/decoder

Fig. 1 outlines the wireless system architecture operating in portrayed conceptual representation of uniformly distributed scattering. For the DC outside-FECC scheme, that is, Fig. 1*a*, the differential encoder (DE) is fed with a *(N/2)*-bit information frame $u = (u_0, \ldots, u_k)$ based on the Bernouli distribution, with the pmf $f(k; p) = p$ if $k = 1$, $(1 - p)$ if $k = 0$, and 0 otherwise. The outer SRCC encoder is fed by either of the DC-coded bit stream (for the case of external DC) or information frame for coherent and internal DC-based systems. The selected half-rate outer SRCC trellis structures for $r \leq 0.33$ and $L \leq 5$ are tabulated in Table 1. The interleaver applies the QP on the bit sequences obtained from the previous step, which is originally proposed in [12, 13] and further developed for serial turbo-like codes in [3–6]. Let $x_{\text{oc.}} = (x_0, \ldots, x_{N-1})$ be a sequence in $\{0, 1\}^N$ which is the N-bit outer system coded sequence. The QP-based interleaver maps the $x_{\text{oc.}}$ to a sequence $\hat{x}_{\text{oc.}} = (x_0, \ldots, x_{N-1})$ according to Theorems I and II of [12] (examples are given in the next section). The inner SRCC encoder is fed with $\hat{x}_{\text{oc.}}$, that is, an N-bit block containing the QP-permutation sequence of outer coded bit stream. The selected inner SRCC trellis structures with $r^{\text{i.}} \in \{0.66, 0.5, 0.4\}$ for $r \leq 0.33$ and $L \leq 5$ are tabulated in Table 1. For the DC inside-FECC scheme, that is, Fig. 1*b*, the DE is fed with a $(N/r^{\text{o.}})$-bit SCQIC-coded sequence. Compared with this scheme, the major advantage of using the DC external to the FECC is that the double-error phenomenon because of the consecutive errors has been eliminated. However, since the system resolution performance depends on the synchroniser circuit of the channel decoder, applying the DC outside FECC is not appropriate for the application to burst mode [9]. The resultant SCQIC can readily be applied to 16-QAM modulation in order to provide a good solution in terms of both power and bandwidth efficiencies. Meanwhile, the low-operating SNR of the resultant STTC increases the transmission robustness to interference and distortion. The QAM modulator maps the DC-SCQICs of $(N/r^{\text{o.}})$-bit blocks to the symbol $\aleph_k$ from the 2^Q-ary constellation set $S = \{\alpha_1, \alpha_2, \ldots, \alpha_{2^Q}\}$, where α_i corresponds to the bit pattern $s_i = \left[s_{i,1}, s_{i,2}, \ldots, s_{i,Q}\right]$ with $s_{i,j} \in \{0, 1\}$. Space-time encoding process follows the wireless transmission sequences for the triplet-antenna systems derived in (37) of [14].

Table 1 CCC structures

Constraint length, L	Overall rate, r	Outer trellis structure and rate, $r^{\text{o.}} = 1/2$	Inner trellis structure and rate, $r^{\text{i.}}$
3	1/3	$G_3^{\text{o.}}$: $\{111, 101\}_2$	$r^{\text{i.}} = 2/3$ $G_3^{\text{i.}}$: $\begin{Bmatrix}111, 101, 000;\\ 000, 111, 101\end{Bmatrix}_2$
	1/4	same as $G_3^{\text{o.}}$	$r^{\text{i.}} = 2/4$ $G_3^{\text{i.}}$: $\begin{Bmatrix}111, 101, 011, 000;\\ 000, 111, 101, 011\end{Bmatrix}_2$
	1/5	same as $G_3^{\text{o.}}$	$r^{\text{i.}} = 2/5$ $G_3^{\text{i.}}$: $\begin{Bmatrix}111, 101, 011, 010, 000;\\ 000, 111, 101, 011, 010\end{Bmatrix}_2$
4	1/3	$G_4^{\text{o.}}$: $\{1111, 1101\}_2$	$r^{\text{i.}} = 2/3$ $G_4^{\text{i.}}$: $\begin{Bmatrix}1111, 1101, 000;\\ 000, 1111, 1101\end{Bmatrix}_2$
	1/4	same as $G_4^{\text{o.}}$	$r^{\text{i.}} = 2/4$ $G_4^{\text{i.}}$: $\begin{Bmatrix}1111, 1101, 1011, 000;\\ 000, 1111, 1101, 1011\end{Bmatrix}_2$
	1/5	same as $G_4^{\text{o.}}$	$r^{\text{i.}} = 2/5$ $G_4^{\text{i.}}$: $\begin{Bmatrix}1111, 1101, 1011, 1001, 000;\\ 000, 1111, 1101, 1011, 1001\end{Bmatrix}_2$
5	1/3	$G_5^{\text{o.}}$: $\{11111, 10001\}_2$	$r^{\text{i.}} = 2/3$ $G_5^{\text{i.}}$: $\begin{Bmatrix}11111, 10001, 00000;\\ 00000, 11111, 10001\end{Bmatrix}_2$
	1/4	same as $G_5^{\text{o.}}$	$r^{\text{i.}} = 2/4$ $G_5^{\text{i.}}$: $\begin{Bmatrix}11111, 10001, 10011, 00000;\\ 00000, 11111, 10001, 10011\end{Bmatrix}_2$
	1/5	same as $G_5^{\text{o.}}$	$r^{\text{i.}} = 2/5$ $G_5^{\text{i.}}$: $\begin{Bmatrix}11111, 10001, 10011, 10111, 00000;\\ 00000, 11111, 10001, 10011, 10111\end{Bmatrix}_2$

This is an open access article published by the IET under the Creative Commons Attribution License (http://creativecommons.org/licenses/by/3.0/)

At the receiver, for detecting symbols of the system, the maximum-likelihood (ML) detector amounts to minimise the decision metrics given in [15], and the resultant sequences are inserted in demodulator block. At the demodulator, the QAM constellations are demapped in order to form the system blocks of SCQIC-coded bit stream, that is, demaps the symbol $\tilde{\aleph}_k$ from the 2^{Q}-ary constellation set S to DC-SCQICs of $(N/r^{o.})$-bit blocks. For the case of the DC internal to FECC, the detected symbols are inserted into the differential decoder (DD) for applying the inverse function of DE, whereas for DC external to FECC the input to the DD is the iteratively decoded SCQIC bit sequences. The demodulator's output has also been computed based on the hard-decision. The system channel values (i.e. soft-decision log-likelihood ratios (LLRs)) have been computed by a separate function at the FEC decoder at the initialisation step of the system iterative decoding.

The DD bit stream inserted into the system SCQIC decoder for recovering the transmitted bits follows near-ML iterative decoding procedure developed for the SCQICs in [6]. Herein, constituent decoders corresponding to SRCC trellis structures iteratively exchange extrinsic information between themselves at the core of the SCQIC iterative decoder architecture. The targeted investigations have been systematically carried out based on the Log-maximum a posteriori (MAP) decoders [8], but the effects of using other decoders for SCQICs are addressed in [6]. For necessary deinterleaving at the decoder architecture, the re-arranged QP feature will be more exploited in Section 4; wherein the samples of the bit streams are scrambled and unscrambled.

3.2 *Wireless system specifications*

We assume rich scattering environments where the receiver antenna responds to each transmitter antenna system through a statistically independent fading coefficient [16], given the wireless transmission is performed using the Gray-coded (GC)-16-QAM. The selected set of the trellis structures for $L \leq 5$ are tabulated in Table 1, supplemented by all extended variants for the FEC rates 1/3, 1/4 and 1/5, that is, every source data bit (or DE data bit in out-DC-FECC) is mapped into three, four and five symbols, respectively. We assume that both the outer and inner SRCCs are terminated by $L - 1$ tail bits in order to drive the encoders to all-zero state. For the half-rate space-time coded system, the measured Doppler spectrum of targeted isotropic scattering mobile radio channel is compared with theoretical Jakes spectrum as in Fig. 2. The signal amplitude received by Rx is affected by the presence of slow-fading Rayleigh flat-fading mechanism and corrupted by additive noise, and follows the channel matrix descriptions as in [2]. The channel modelling analysis has employed the stochastic system models, and considers the generic probability density function (PDF) of the field strength in the intended wireless link. Therefore, the bandlimited impulse response for the three slow-fading links is depicted in Fig. 3, in order to clearly demonstrate the link's impulse response in the proposed analytical case of 3 × 1 links along with the given specifications without affecting the overall system BER performance. It is also assumed that the stationary scatters are on average distributed uniformly on a circle around the receiver with omnidirectional antenna, with the same average power from all directions. Invoking the central limit theorem, we can assume that power from one direction is complex Gaussian distributed. In addition, the technical issues related to the intended stochastic multiple antenna channel modelling tackles the same procedure as given in [2, 6].

If we assume that the receiver moves with a certain speed, the number of components coming from each direction will take the tub form of Jakes spectrums, given analytically by $S_D(v) = (1/\pi.\ v_{\max}).(1 - (v/v_{\max})^2)^{-1/2}$ for $-v_{\max} \leq v \leq v_{\max}$ [17], where $f_{\max}$ is the maximum Doppler-shift. The scatters are equally distributed in all directions and the receiver is also moving. The radio signal from all directions has on average the same power and delay. The spectrum can be interpreted such that infinite contributions, which are very small, come from 0 and 180°, which creates two singularities in $v_{\max}$ and $-v_{\max}$.

4 Numerical results and discussion

In this section, representative wireless system performance evaluation results have been used in order to characterise the attainable

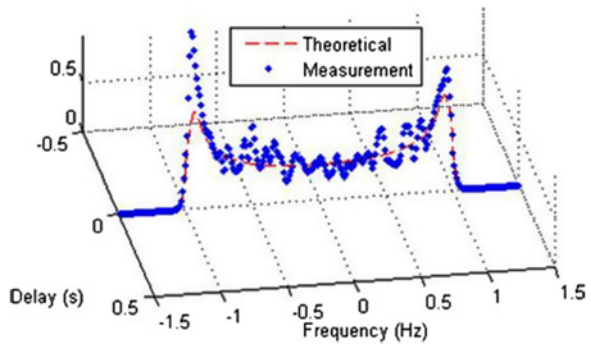

Fig. 2 *Computed theoretical against measured Jakes Doppler spectra of a path against path delay(s) in one branch of wireless MISO mobile radio link*

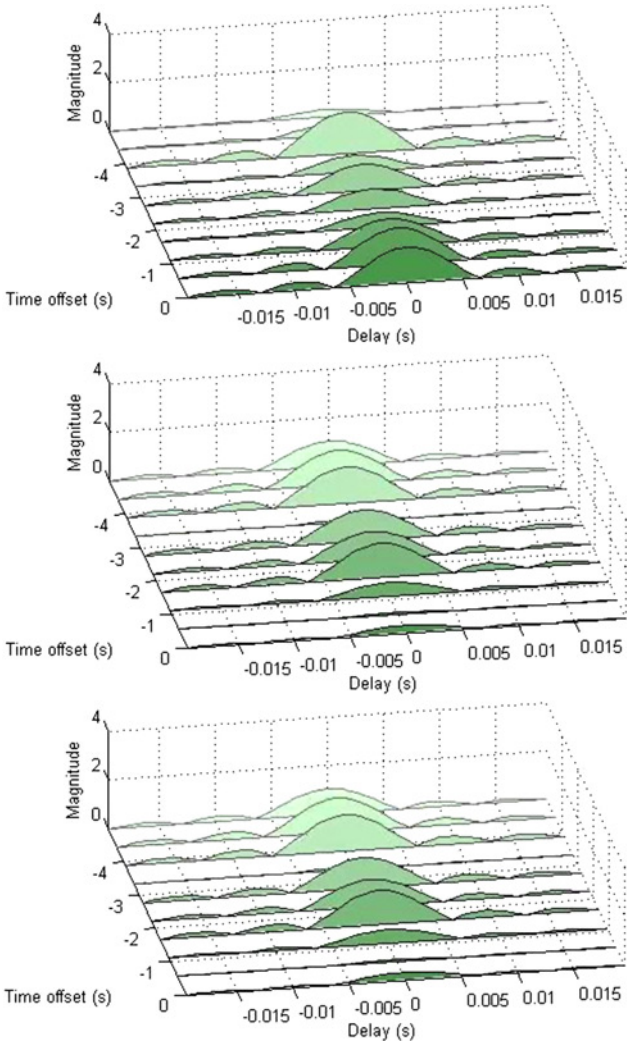

Fig. 3 *Snapshots of computed bandlimited impulse response for the three slow-fading quasi-static wireless MISO mobile radio links; the darkest curve presenting the current response at BER = 1.778e − 4 and E_b/N_0 = 4 dB*

This is an open access article published by the IET under the Creative Commons Attribution License (http://creativecommons.org/licenses/by/3.0/)

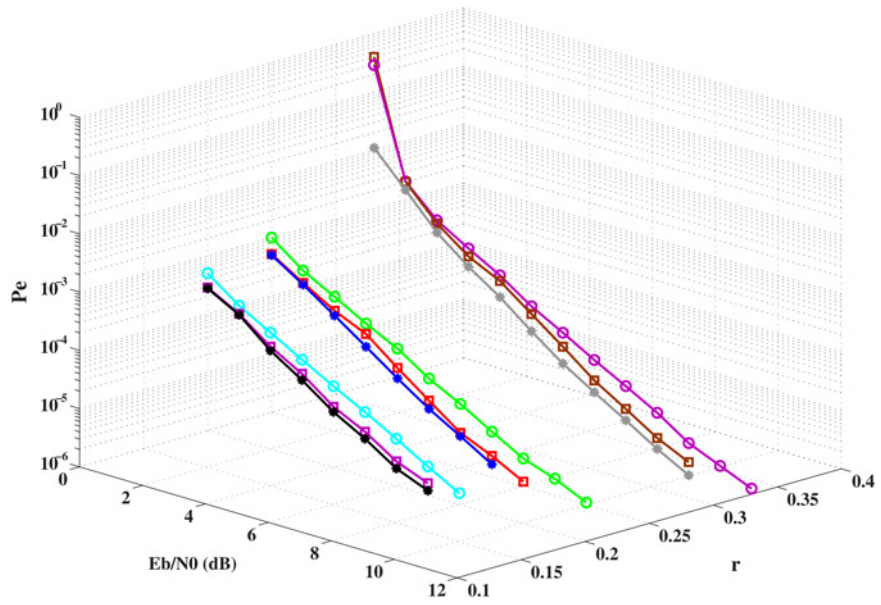

Fig. 4 *Comparison of BER against E_b/N_0 against r for the coherent wireless systems*

performance of the coded multiple-input–single-output (MISO) systems from the aspects outlined in Section 1. In Figs. 4–6, the BER is shown against the energy per bit/noise power spectral density (E_b/N_0) and the FEC rate (r) for coherent, out-FECC DC and in-FECC DC systems. Herein, the lines with circle, square and star markers present the performance curves associated with employing $L = 3$, 4 and 5. The particular generator polynomials are chosen so that the designed SCQIC does not have catastrophic error propagation and has high free distance for the selected FEC rates and the constraint lengths. Meanwhile, FEC rates and component code constraint lengths are chosen from among the most widely used range for provisioning overall design tradeoff. As it can be seen, the huge difference in performance that can result from extra parity bit as a result of lowering FEC rate is on average of 2 dB when the comparison is made for fixed-length CCCs with the same trellis structure.

For $r = 1/3 \rightarrow 1/5$ coding gains of up to $\simeq 4$ dB are achieved at the expense of spectral efficiency degradations because of two extra parity bits.

The performance improvement due to employing the CCCs with the higher L becomes not outstandingly significant, and suggests to limit the $L < 6$ in order to avoid the considerable increase in system decoding complexities which does not result in worthwhile BER reduction, neither in waterfall-region, nor in flare region; that is, based on [8], increasing the L by a factor one (e.g. L: $3 \rightarrow 4$ or L: $4 \rightarrow 5$) requires around two times more additions, multiplications and maximisation operations when Max-Log-MAP algorithm is employed at the iterative decoder, while yield performance gains around 1 dB according to Figs. 4–6 for attaining BER $\simeq 10^{-6}$. As far as the Log-MAP algorithm is a more interesting candidate to be used for yielding performance close to original MAP decoders by using correction function, the number of lookups required for

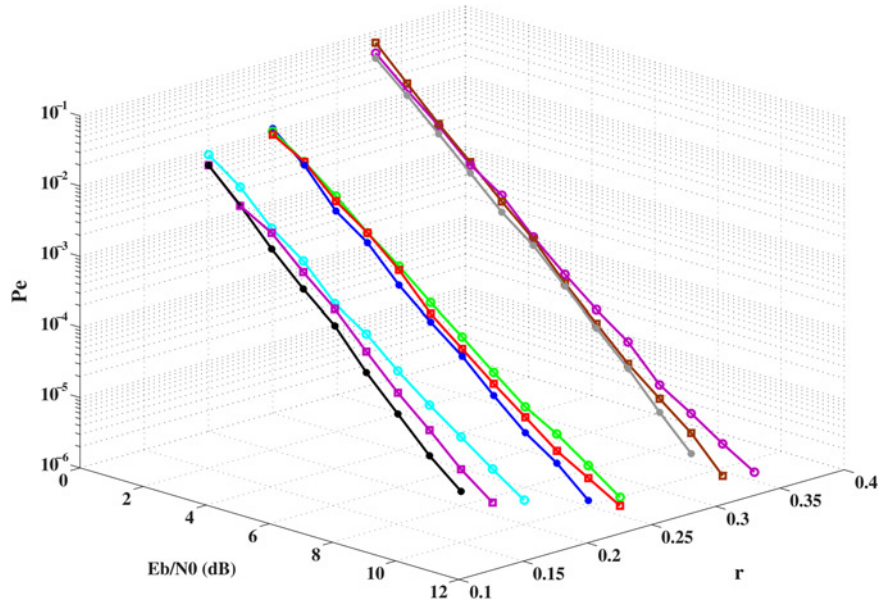

Fig. 5 *Comparison of BER against E_b/N_0 against r for the wireless system with out-DC-FECC*

This is an open access article published by the IET under the Creative Commons Attribution License (http://creativecommons.org/licenses/by/3.0/)

doi: 10.1049/joe.2014.0001

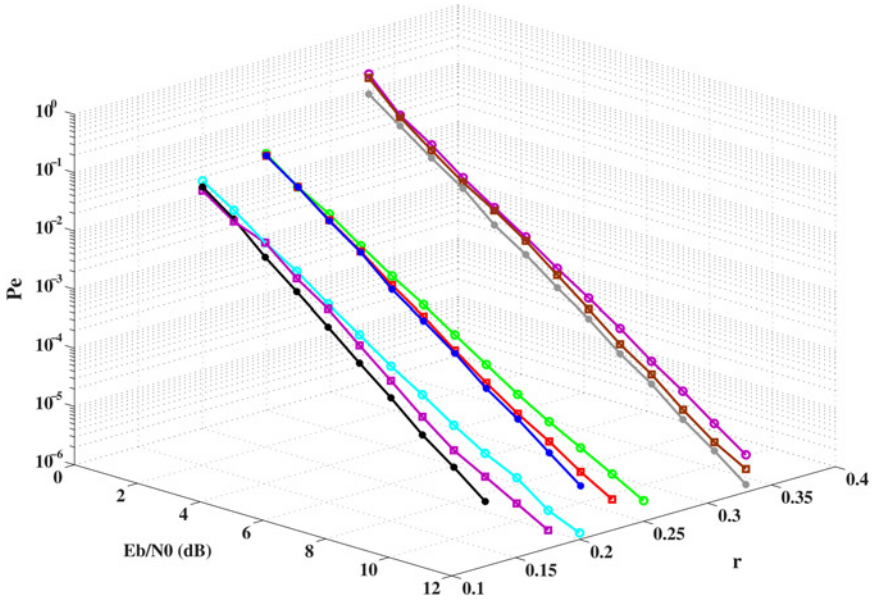

Fig. 6 *Comparison of BER against E_b/N_0 against r for the wireless system with in-DC-FECC*

computing correction function brings further operations for the practical use of high constraint lengths.

As be seen from the performance curves, since for DC-in-FECC one erroneously detected phase will cause two successive false symbols even if the next phase is received correctly, that is, double-error phenomenon, the error burst causes serious BER degradation of above 2 dB compared with the coherent systems. For reducing the highly correlated errors, in DC-out-FECC scheme, the SCQIC decoder does not encounter the double-error phenomenon and only the BER of SCQIC decoder output is doubled. Hence, doubling the SCQIC decoder BER yields a smaller coding gain loss at the expense of using synchroniser circuit for SCQIC decoder, which is not suitable for applications where long delay for resolving the phase ambiguity cannot be tolerated [9].

The effects of changing the structure of the QP-vectors and their lengths have been examined in this part. For instance, according to design Theorems I and II of [12], the QP-vectors for $N = 16$ and 32 are given as follows, where $\pi_N^{(C,F)}$ denotes the vector associated with QP-length N, with cyclic shift C and multiplicative factor F (see equation at the bottom of the next page).

Hence, for instances of 16-/32-bit permutation lengths, the QP-based interleaver maps generated sequences from half-rate outer SRCC trellis structures for $r \leq 0.33$ and $L \leq 5$, for example

$$\rightarrow \bar{v} = \langle 1110001010011000\rangle_{16}$$
$$\rightarrow \bar{v} = \langle 11100010100110001110001010011000\rangle_{32}$$

Into the reordered sequences of w_C^F given as follows:

For π_{16} (see equation at the bottom of next page)

For π_{32}
(see equation at the bottom of next page)

For the case of message passing between the component decoders corresponding to outer/inner SRCC trellis structures, the input of outer decoder from the output of inner decoder utilises the inverse of this function at the deinterleaver. Instances of the QP-based deinterleaving are given as follows, where the $\tilde{w}_C^F$ is an

$$\pi_N^{(C,F)}:\begin{cases}\pi_{16}:\begin{cases}\pi^{1,F\in\{1:15\}_{\text{odd}}}:\begin{cases}\pi^{1,1}=[4,\ 15,\ 7,\ 14,\ 13,\ 11,\ 3,\ 1,\ 9,\ 16,\ 10,\ 5,\ 8,\ 12,\ 6,\ 2]\\ \cdots\\ \pi^{1,15}=[12,\ 6,\ 10,\ 13,\ 8,\ 2,\ 9,\ 1,\ 15,\ 7,\ 5,\ 4,\ 11,\ 3,\ 14,\ 16]\end{cases}\\ \cdots\\ \pi^{15,F\in\{1:15\}_{\text{odd}}}:\begin{cases}\pi^{15,1}=[6,\ 2,\ 4,\ 15,\ 7,\ 14,\ 13,\ 11,\ 3,\ 1,\ 9,\ 16,\ 10,\ 5,\ 8,\ 12]\\ \cdots\\ \pi^{15,15}=[14,\ 16,\ 12,\ 6,\ 10,\ 13,\ 8,\ 2,\ 9,\ 1,\ 15,\ 7,\ 5,\ 4,\ 11,\ 3]\end{cases}\end{cases}\\ \pi_{32}:\begin{cases}\pi^{1,F\in\{1:31\}_{\text{odd}}}:\begin{cases}\pi^{1,1}=[4,\ 15,\ 7,\ 14,\ 32,\ 11,\ 30,\ 26,\ 25,\ 16,\ 31,\ 6,\ 24,\ 28,\ 22,\ 1,\ 17,\ 8,\ 18,\ 13,\ 29,\ 20,\\ \quad 3,\ 9,\ 12,\ 23,\ 10,\ 5,\ 21,\ 19,\ 27,\ 2]\\ \cdots\\ \pi^{1,31}=[7,\ 15,\ 13,\ 29,\ 24,\ 11,\ 22,\ 25,\ 31,\ 14,\ 5,\ 21,\ 16,\ 26,\ 17,\ 1,\ 12,\ 6,\ 10,\ 28,\ 3,\ 18,\\ \quad 9,\ 8,\ 4,\ 23,\ 2,\ 20,\ 27,\ 19,\ 30,\ 32]\end{cases}\\ \cdots\\ \pi^{31,F\in\{1:31\}_{\text{odd}}}:\begin{cases}\pi^{31,1}=[27,\ 2,\ 4,\ 15,\ 7,\ 14,\ 32,\ 11,\ 30,\ 26,\ 25,\ 16,\ 31,\ 6,\ 24,\ 28,\ 22,\ 1,\ 17,\ 8,\ 18,\ 13,\ 29,\\ \quad 20,\ 3,\ 9,\ 12,\ 23,\ 10,\ 5,\ 21,\ 19]\\ \cdots\\ \pi^{31,31}=[30,\ 32,\ 7,\ 15,\ 13,\ 29,\ 24,\ 11,\ 22,\ 25,\ 31,\ 14,\ 5,\ 21,\ 16,\ 26,\ 17,\ 1,\ 12,\ 6,\ 10,\ 28,\\ \quad 3,\ 18,\ 9,\ 8,\ 4,\ 23,\ 2,\ 20,\ 27,\ 19]\end{cases}\end{cases}\end{cases}$$

This is an open access article published by the IET under the Creative Commons Attribution License (http://creativecommons.org/licenses/by/3.0/)

arbitrary sequence

$$\tilde{w}_5^5 = \langle 1110001010011000\rangle_{16} \xrightarrow{\pi^{-1}} \langle 0001010111000101\rangle_{16}$$
$$\tilde{w}_{21}^{21} = \langle 11100010100110001010001010010101\rangle_{32} \xrightarrow{\pi^{-1}} \langle 10101001000000001100011011110101\rangle_{32}$$

As it has been shown, for the case of permutations with different *Fs* and *Cs*, different randomisation mappings can be constructed. In Fig. 7, these variations have been investigated for the high gain $N = 1024$ system, where the F and C are chosen in mid-range of different size categories. So, when either of F or C is varying, the other is fixed to its mid-range value. As it can be seen, as far as the gain gaps are negligible, the selection of structural parameters for construction of QPs makes no significant BER superiority/inferiority.

In the classic turbo coding and its subsequent contributions, exceptional coding gains have been reported to be attained in the case of employing long permutations, that is, N exceeds 10 000 bits such as, for example, Berrou's classic half-rate PCCCing with $N = 65\,536$ bits. However, since the extra complexity and delay are not jus-

$$w_{1:15}^1: \begin{Bmatrix} \langle 0010101110000101\rangle \\ \langle 0101011100001010\rangle \\ \langle 1010111000010100\rangle \\ \langle 0101110000101001\rangle \\ \langle 1011100001010010\rangle \\ \langle 0111000010100101\rangle \\ \langle 1110000101001010\rangle \\ \langle 1100001010010101\rangle \\ \langle 1000010100101011\rangle \\ \langle 0000101001010111\rangle \\ \langle 0001010010101110\rangle \\ \langle 0010100101011100\rangle \\ \langle 0101001010111000\rangle \\ \langle 1010010101110000\rangle \\ \langle 0100101011100001\rangle \end{Bmatrix} \cdots w_{1:15}^5: \begin{Bmatrix} \langle 0101000111001100\rangle \\ \langle 1010001110011000\rangle \\ \langle 0100011100110001\rangle \\ \langle 1000111001100010\rangle \\ \langle 0001110011000101\rangle \\ \langle 0011100110001010\rangle \\ \langle 0111001100010100\rangle \\ \langle 1110011000101000\rangle \\ \langle 1100110001010001\rangle \\ \langle 1001100010100011\rangle \\ \langle 0011000101000111\rangle \\ \langle 0110001010001110\rangle \\ \langle 1100010100011100\rangle \\ \langle 100010100011100\rangle \\ \langle 000101000111001\rangle \end{Bmatrix} \cdots w_{1:15}^{15}: \begin{Bmatrix} \langle 1001011101000100\rangle \\ \langle 0010111010001001\rangle \\ \langle 0101110100010010\rangle \\ \langle 1011101000100100\rangle \\ \langle 0111010001001001\rangle \\ \langle 1110100010010010\rangle \\ \langle 1101000100100101\rangle \\ \langle 1010001001001011\rangle \\ \langle 0100010010010111\rangle \\ \langle 1000100100101110\rangle \\ \langle 0001001001011101\rangle \\ \langle 0010010010111010\rangle \\ \langle 0100100101110100\rangle \\ \langle 1001001011101000\rangle \\ \langle 0010010111010001\rangle \end{Bmatrix}$$

$$w_{1:31}^1: \begin{Bmatrix} \langle 0010000010000101101110111111000101\rangle \\ \langle 0100000100001011011101111110001010\rangle \\ \langle 1000001000010110111011111100010100\rangle \\ \langle 0000010000101101110111111000101001\rangle \\ \langle 0000100001011011101111100010100100\rangle \\ \langle 0001000010110111011111000101001000\rangle \\ \langle 0010000101101110111110001010010000\rangle \\ \langle 0100001011011101111100010100100000\rangle \\ \langle 0000101101110111110001010010000001\rangle \\ \langle 0001011011101111100010100100000010\rangle \\ \langle 0010110111011111000101001000000100\rangle \\ \langle 0101101110111110001010010000001000\rangle \\ \langle 1011011101111100010100100000010000\rangle \\ \langle 0110111011110001010010000001000001\rangle \\ \langle 1101110111100010100100000010000010\rangle \\ \langle 1011101111000101001000000100000101\rangle \\ \langle 0111011110001010010000001000001011\rangle \\ \langle 1110111100010100100000010000010110\rangle \\ \langle 1101111000101001000000100000101101\rangle \\ \langle 1011110001010010000001000001011011\rangle \\ \langle 0111100010100100000010000010110111\rangle \\ \langle 1111000101001000001000001011011110\rangle \\ \langle 1110001010010000010000010110111101\rangle \\ \langle 1100010100100000100000101101110111\rangle \\ \langle 1000101001000001000001011011101111\rangle \\ \langle 0001010010000010000010110111011111\rangle \\ \langle 0010100100000100000101101110111110\rangle \\ \langle 0101001000001000010110111011111100\rangle \\ \langle 1010010000010000101101110111111000\rangle \\ \langle 0100100000100001011011101111000001\rangle \end{Bmatrix} \cdots w_{1:31}^{11}: \begin{Bmatrix} \langle 1010000101100001110101000000101111\rangle \\ \langle 0100001011000011101000000101111\rangle \\ \langle 1000010110000111010000001011110\rangle \\ \langle 0000101100001110100000010111101\rangle \\ \langle 0001011000011101000000101111010\rangle \\ \langle 0010110000111010000010111110100\rangle \\ \langle 0101100001110100000010111101000\rangle \\ \langle 1011000011101000000101111010000\rangle \\ \langle 0110000111010000010111110100001\rangle \\ \langle 1100001110100000010111110100010\rangle \\ \langle 1000011101000000101111101000101\rangle \\ \langle 0000111010000001011111010000101\rangle \\ \langle 0001110100000010111110100001011\rangle \\ \langle 0011101000000101111101000010110\rangle \\ \langle 0111010000001011111010000101100\rangle \\ \langle 1110100000010111110100001011000\rangle \\ \langle 1101000000101111101000010110000\rangle \\ \langle 1010000001011111010000101100001\rangle \\ \langle 0100000010111110100001011000011\rangle \\ \langle 1000000101111101000010110000111\rangle \\ \langle 0000001011111010000101100001101\rangle \\ \langle 0000010111110100001011000011010\rangle \\ \langle 0000101111101000010110000111001\rangle \\ \langle 0001011111010000101100001110100\rangle \\ \langle 0010111110100001011000011101000\rangle \\ \langle 0101111010000101100001110100000\rangle \\ \langle 1011111010000101100001110100000\rangle \\ \langle 0111110100001011000011101000001\rangle \\ \langle 1111101000010110000111010000010\rangle \\ \langle 1111010000101100001110100000101\rangle \\ \langle 1110100001011000011101000000101\rangle \end{Bmatrix}$$

This is an open access article published by the IET under the Creative Commons Attribution License (http://creativecommons.org/licenses/by/3.0/)

doi: 10.1049/joe.2014.0001

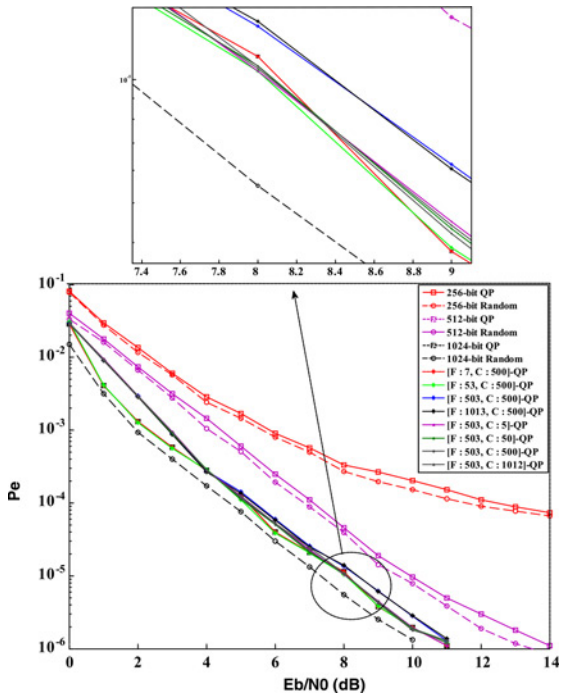

Fig. 7 *Comparison of BER curves for QP-/random-based interleaved wireless systems with* $200 \simeq < N \simeq < 1000$*; comparison of gain gaps between QP-based systems for selected cycle shifts (Cs) and multiplicative factors (Fs)*

tified for modern wireless applications, the fundamental design issues of channel codes directed a great deal of efforts for designing short-length FECs; that is, adopting short-frame system structures at expense of BER degradations. Hence, this design guideline limits our investigation to be conducted for range $N \simeq < 1000$ bits; that is, for the comparative investigation between the QP and the random permutations' gain gaps for different lengths because of the reason discussed in (4) of the outlined list in Section 2. Fig. 7 further shows the performance curves as a function of interleaver size, which presents how performance improves as the interleaver length increases for $N_{\mathrm{INT}} \simeq < 1000$. The following important observations can be made from the obtained results: (i) As far as the QP- and random-based systems are operating in close SNRs, that is, gain gaps for yielding similar BER are not high for the three possible interleaver lengths in $200 \simeq < N \simeq < 1000$ range (i.e. $N \in \{256, 512, 1024\}$) the research suggests to employ QPs for modern short-frame applications which also require lower implementation complexities. (ii) For the three possible and selected N_s which satisfy both QP construction conditions and $N \simeq < 1000$, 256 bit scheme is not capable of operating without an error floor. Whereas the 512 bit scheme is provisioning the BER performance in both waterfall and flare regions, and reduces the further complexities associated with the high gain $N = 1024$ bit scheme.

5 Conclusion

In this paper, in order to contrive an attractive design tradeoff for the QP-based STTCs, algebraic permutation and SRCC component code design issues and FEC-rate flexibility, which have dramatic

$$\cdot w_{1:31}^{21}: \begin{cases} \langle 0001101011100001011100011000 1100\rangle \\ \langle 0011010111000010111000110001 1000\rangle \\ \langle 0110101110000101110001100011 0000\rangle \\ \langle 1101011100001011100011000110 0000\rangle \\ \langle 1010111000010111000110001100 0001\rangle \\ \langle 0101110000101110001100011000 0011\rangle \\ \langle 1011100001011100011000110000 0110\rangle \\ \langle 0111000010111000110001100000 1101\rangle \\ \langle 1110000101110001100011000001 1010\rangle \\ \langle 1100001011100011000110000011 0101\rangle \\ \langle 1000010111000110001100000110 1011\rangle \\ \langle 0000101110001100011000001101 0111\rangle \\ \langle 0001011100011000110000011010 1110\rangle \\ \langle 0010111000110001100000110101 1100\rangle \\ \langle 0101110001100011000001101011 1000\rangle \\ \langle 1011100011000110000011010111 0000\rangle \\ \langle 0111000110001100000110101110 0001\rangle \\ \langle 1110001100011000001101011100 0010\rangle \\ \langle 1100011000110000011010111000 0101\rangle \\ \langle 1000110001100000110101110000 1011\rangle \\ \langle 0001100011000001101011100001 0111\rangle \\ \langle 0011000110000011010111000010 1110\rangle \\ \langle 0110001100000110101110000101 1100\rangle \\ \langle 1100011000001101011100001011 1000\rangle \\ \langle 1000110000011010111000010111 0001\rangle \\ \langle 0001100000110101110000101111 0011\rangle \\ \langle 0011000001101011100001011110 0110\rangle \\ \langle 0110000011010111000010111000 1100\rangle \\ \langle 1100000110101110000101110001 1000\rangle \\ \langle 1000001101011100001011100011 0001\rangle \\ \langle 0000011010111000010111000110 0011\rangle \end{cases} \cdots w_{1:31}^{31}: \begin{cases} \langle 1011000100000011100111001100 100\rangle \\ \langle 0110001000000111001111001100 1001\rangle \\ \langle 1100010000001110011110011001 0010\rangle \\ \langle 1000100000011100111100110010 0101\rangle \\ \langle 0001000000111001111001100100 1011\rangle \\ \langle 0010000001110011110011001001 0110\rangle \\ \langle 0100000011100111100110010010 1100\rangle \\ \langle 1000000111001111001100100101 1000\rangle \\ \langle 0000001110011110011001001011 0001\rangle \\ \langle 0000011100111100110010010110 0010\rangle \\ \langle 0000111001111001100100101100 0100\rangle \\ \langle 0001110011110011001001011000 1000\rangle \\ \langle 0011100111100110010010110001 0000\rangle \\ \langle 0111001111001100100101100010 0000\rangle \\ \langle 1110011110011001001011000100 0000\rangle \\ \langle 1100111100110010010110001000 0001\rangle \\ \langle 1001111001100100101100010000 0011\rangle \\ \langle 0011110011001001011000100000 0111\rangle \\ \langle 0111100110010010110001000000 1110\rangle \\ \langle 1111001100100101100010000001 1100\rangle \\ \langle 1110011001001011000100000011 1001\rangle \\ \langle 1100110010010110001000000111 0011\rangle \\ \langle 1001100100101100010000001110 0111\rangle \\ \langle 0011001001011000100000011100 1111\rangle \\ \langle 0110010010110001000000111001 1110\rangle \\ \langle 1100100101100010000001110011 1100\rangle \\ \langle 1001001011000100000011100111 1001\rangle \\ \langle 0010010110001000000111001111 0011\rangle \\ \langle 0100101100010000001110011111 0110\rangle \\ \langle 1001011000100000011100111110 0100\rangle \\ \langle 0010110001000000111001111001 1001\rangle \end{cases}$$

This is an open access article published by the IET under the Creative Commons Attribution License (http://creativecommons.org/licenses/by/3.0/)

effect on the free distance of the resultant STTC method, have been all addressed and characterised when they are all amalgamated. The results of this paper can be extended in a number of ways which are of great theoretical and practical interest, including investigation on the potential enhancements as a result of deploying directional antennas at one or both ends of the MISO radio link, and investigation over mobile-to-mobile scattering propagation environments.

6 References

[1] Bauch G.: 'Concatenation of space-time block codes and turbo-TCM'. IEEE Int. Conf. Communications (ICC), June 1999, vol. 2, pp. 1202–1206

[2] Mehran F., Maunder R.G.: 'Wireless MIMO systems employing joint turbo-like STBC codes with bit-level algebraically-interleaved URSCs'. IEEE Int. Wireless Symp. (IWS), April 2013, pp. 1–4

[3] Mehran F., Rahimian A.: 'Physical layer performance enhancement for femtocell SISO/MISO soft real-time wireless communication systems employing serial concatenation of quadratic interleaved codes'. 20th Iranian Conf. Electrical Engineering (ICEE), May 2012, pp. 1188–1193

[4] Rahimian A., Mehran F.: 'BEP enhancement for semi-femtocell MIMO systems employing SC-QICs and OSTBCs', *Int. J. Electron. Commun. Comput. Technol.*, 2013, **3**, (1), pp. 329–332

[5] Rahimian A., Mehran F.: 'Short-length FSU-SCQICs over coherent and incoherent stochastic aeronautical MISO channels'. 19th Asia-Pacific Conf. Communications (APCC), August 2013, pp. 655–656

[6] Rahimian A., Mehran F., Maunder R.G.: 'Serial concatenation of quadratic interleaved codes in different wireless Doppler environments'. IEEE Fourth Int. Conf. Electronics Information and Emergency Communication (ICEIEC), November 2013, pp. 94–101

[7] Hanzo L., Woodard J.P., Robertson P.: 'Turbo decoding and detection for wireless applications', *Proc. IEEE*, 2007, **95**, (6), pp. 1178–1200

[8] Rahimian A., Mehran F., Maunder R.G.: 'Joint space-time algebraically-interleaved turbo-like coded incoherent MIMO systems with optimal and suboptimal MAP probability decoders'. IEEE Fourth Int. Conf. Electronics Information and Emergency Communications (ICEIEC), November 2013, pp. 1–8

[9] Nguyen T.M.: 'Phase-ambiguity resolution for QPSK modulation systems'. JPL Publication 89–4, Part I: A Review, May 1989, pp. 1–25

[10] Jung P., Nasshan M.: 'Dependence of the error performance of turbo-codes on the interleaver structure in short frame transmission systems', *Electron. Lett.*, 1994, **30**, (4), pp. 287–288

[11] Dogandzic A., Zhang B.: 'Estimating Jakes' Doppler power spectrum parameters using the Whitte approximation', *IEEE Trans. Signal Process.*, 2005, **53**, (3), pp. 987–1005

[12] Takeshita O.Y., Costello D.J.: 'New classes of algebraic interleavers for turbo-codes'. IEEE Int. Symp. Information Theory (ISIT), August 1998

[13] Takeshita O.Y., Costello D.J.: 'New deterministic interleaver designs for turbo codes', *IEEE Trans. Inf. Theory*, 2000, **46**, (6), pp. 1988–2006

[14] Tarokh V., Jafarkhani H., Calderbank A.: 'Space-time block codes from orthogonal designs', *IEEE Trans. Inf. Theory*, 1999, **45**, pp. 1456–1467

[15] Tarokh V., Jafarkhani H., Calderbank A.: 'Space-time block coding for wireless communications: performance results', *IEEE J. Sel. Areas Commun.*, 1999, **17**, pp. 451–460

[16] Clarkson K.L., Sweldens W., Zheng A.: 'Fast multiple-antenna differential decoding', *IEEE Trans. Commun.*, 2001, **49**, (2), pp. 253–261

[17] Jakes W.C.: 'Microwave mobile communications' 2nd edition (Wiley, New York, 1974)

This is an open access article published by the IET under the Creative Commons Attribution License (http://creativecommons.org/licenses/by/3.0/)

doi: 10.1049/joe.2014.0001